Supplemental Data

Cortical circuit model. Since the "→" and "←" presynaptic cells are equivalent in the model, the description will only be given for "→" cells below. The intracellular voltage of the *j*th "→" cell at time *t*, $V_j^{\rightarrow}(t)$, was determined by: $\tau_0 \frac{\partial V_j^{\rightarrow}(t)}{\partial t} + V_j^{\rightarrow}(t) = V_j^{\rightarrow,IN}(t)$, where τ_0 (2 ms) is the membrane time constant of the cell, and $V_j^{\rightarrow,IN}$ represents the synaptic input to the cell in response to visual stimuli (see below). The intracellular voltage of the target neuron (black circle), $V_c(t)$, was determined by:

$$\tau_0 \frac{\partial V_c(t)}{\partial t} + V_c(t) = V_c^{nd}(t) + \sum_{j=1}^{j=143} \int_0^{\infty} S_j^{\rightarrow} R_j^{\rightarrow}(t-\tau) F(\tau) d\tau + \sum_{j=1}^{j=143} \int_0^{\infty} S_j^{\leftarrow} R_j^{\leftarrow}(t-\tau) F(\tau) d\tau$$

where V_c^{nd} represents the non-direction-selective input in response to visual stimuli (but making it direction-selective does not change the conclusions, see below), $S_j^{\rightarrow}$ represents connection strength from the *j*th "→"cell, and $R_j^{\rightarrow}$ is the firing rate of the cell, proportional to the rectified intracellular voltage: $R_j^{\rightarrow}(t) = \alpha\left[V_j^{\rightarrow}(t) - V_t\right]^+$ (V_t = 0.2 is the spiking threshold and α = 0.7 ms^{-1} is a scaling constant); the actual spike train was generated with a rate modulated Poisson process (same for the target neuron). F represents the impulse response of the synaptic input: $F(t) = c^2 t e^{-ct}$ (c = 0.5 ms^{-1}, which controls the time course of synaptic response).

The initial synaptic connections from both the "→" and "←" cells followed

Gaussian distributions: $S_j^{\rightarrow} = e^{-x_j^{\rightarrow 2}/2\sigma_s^2}$, where $x_j^{\rightarrow}$ is the RF center position of the *j*th "$\rightarrow$" neuron (RF center of the target cell is defined as 0), and σ_s (1.0^o) determines the width of the distribution. To implement STDP at these connections, the synaptic strength changed after each pair of pre- and postsynaptic spikes according to: $S_j^{\rightarrow}(n) = S_j^{\rightarrow}(n-1)(1+\Delta S)$, where $S_j^{\rightarrow}(n)$ is the synaptic strength after the *n*th pair of spikes. $\Delta S = \begin{cases} A_+ e^{-|\Delta t|/\tau_+} & if \quad \Delta t \geq 0 \\ A_- e^{-|\Delta t|/\tau_-} & if \quad \Delta t < 0 \end{cases}$, where Δt is the inter-spike interval (> 0 if pre preceding post), τ_+ (14.8 ms) and τ_- (33.8 ms) are the time constants for the potentiation and depression windows, respectively, measured experimentally for layer 2/3 intracortical connections in the visual cortex (Froemke and Dan, 2002). A_+ (4.7×10^{-4}) and A_- (-4.9×10^{-4}) are the scaling factors, which were set to be 4% of the experimentally measured values to slow down training and therefore to reduce simulation noise due to the stochastic nature of the spike trains. To simulate development of the circuit, we presented spatially localized visual stimuli sweeping across the visual field (**Fig. 6B**). The input to the *j*th "$\rightarrow$"cell was determined by $V_j^{\rightarrow,IN}(t) = g^{\rightarrow} e^{-(vt - x_j^{\rightarrow})^2/2\sigma^2}$, where g controls the direction selectivity of the cell: $g^{\rightarrow} = 1$ for rightward stimulus and $g^{\rightarrow} = 0.4$ for leftward stimulus; v is the velocity of the stimulus, $x_j^{\rightarrow}$ is the RF center position, and σ (0.85^o) determines the RF size. The non-direction-selective input to the target neuron was determined by $V_c^{nd}(t) = g_c e^{-(vt)^2/2\sigma^2}$, where g_c (0.5) controls the strength of the input (see below for discussion on response latency).

To simulate the response of the target cell to a stationary stimulus at position *x*

containing motion signals (**Fig. 5A**), the inputs to the circuits were determined by $V_j^{\rightarrow,IN}(x) = g^{\rightarrow} e^{-(x-x_j^{\rightarrow})^2/2\sigma^2}$ (with σ = 0.85° and $g^{\rightarrow}$ dependent on the direction of motion, see above) and $V_c^{nd}(x,t) = g_c e^{-x^2/2\sigma^2}$. The RF of the target cell was then represented as the simulated response as a function of *x*.

Cortical adaptation (**Fig. 5B**) was simulated as in a previous study (Felson et al., 2002). Briefly, the firing rate of each neuron was scaled by an adaptation factor $A_j^{\rightarrow}$ ($R_j^{\rightarrow}(t)$ replaced by $A_j^{\rightarrow}(t)R_j^{\rightarrow}(t)$ in the above equations). $A_j^{\rightarrow}$ was reduced each time the neuron spiked: $A_j^{\rightarrow} \rightarrow A_j^{\rightarrow}[1 - c_a R_j^{\rightarrow}(t_0)]$, where $R_j^{\rightarrow}(t_0)$ is the firing rate of the neuron at time t_0, and c_a (0.5) determines the magnitude of adaptation. Before stimulus onset, *A* was set to 1 for all neurons.

The parameters in the model were chosen to illustrate the effects qualitatively rather than to match the experimental data. All the predictions presented in this study were robust and insensitive to the exact model parameters. The asymmetric circuit can still form when the moving targets (**Fig. 6B**) are considerably larger than the RFs, and including non-direction-selective presynaptic neurons in the model did not change the predictions qualitatively.

Direction selectivity of the target cell. Although in the above model the target neuron exhibited no direction selectivity, making it direction selective (by replacing V_c^{nd} with a direction-selective term) does not change the predictions qualitatively. **Fig. S1** shows the result of a simulation. The target neuron was direction selective prior to the development

of the asymmetric circuit (same as the "←" presynaptic neurons). After extensive exposure to motion stimuli in both directions, the STDP mechanism led to a spatial asymmetry in both the "→" and "←" connections (**Fig. S1a**). For this direction-selective target neuron, motion signal in a stationary test stimulus caused a displacement of the RF in the opposite direction (**Fig. S1b**), whereas motion adaptation induced a shift of the RF in the direction of adaptation (**Fig. S1c**). Thus, the effects of motion and motion adaptation on RF position are similar for directionally selective and non-selective target neurons. Experimentally, these effects were also found for cells with a wide range of direction selectivity (from 0 to 0.87; also see **Fig. 1B,** the first and last cells in the bottom row are clearly direction selective).

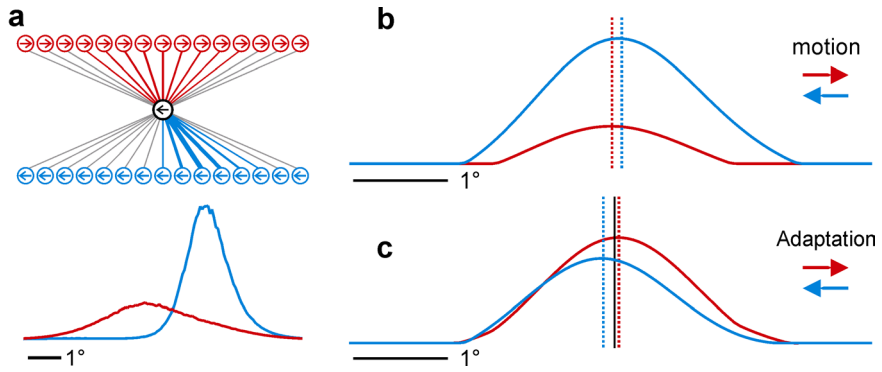

Fig. S1. Asymmetric circuit with the target neuron preferring leftward motion. **a**, Mature circuit after extensive exposure to balanced leftward and rightward motion stimuli. Upper panel: circuit diagram, with line thickness proportional to connection strength. Lower panel: synaptic strength as a function of presynaptic RF position. The initial connections were symmetric, same as in **Fig. 6A**. **b**, Effect of motion signal in the test stimulus on RF position. Solid curves: RFs of the target neuron measured with test stimulus containing rightward (red) and leftward (blue) motion signal. Dotted vertical lines indicate RF center positions. **c**, Effect of motion adaptation on RF position. Solid curves: RFs of the target neuron following rightward (red) and leftward (blue) adaptation. Vertical lines indicate RF center positions before adaptation (black solid), after rightward adaptation (red dotted), and after leftward adaptation (blue dotted). Note that leftward adaptation caused a larger shift (from the black vertical line) than rightward adaptation.

Note that, in addition to the spatial asymmetry, the mature circuit also exhibited a clear difference between the "→" and "←" connections in their overall strength (their initial strengths were the same, as in **Fig. 6A**). The "←" connections became stronger than the "→" connections, and this can further enhance the direction selectivity of the target cell. Interestingly, because the direction-selective target cell received stronger inputs from presynaptic cells preferring the same direction, adaptation in the preferred direction caused a larger RF shift than adaptation in the non-preferred direction (**Fig. S1c**). To compare this prediction with the experimental data, for each cell we computed RF shifts induced by adaptation in the preferred and the non-preferred directions separately. For the 56 cells analyzed, adaptation in the preferred direction caused a 2.5±0.8% shift in RF position (measured within 48s after adaptation), and adaptation in the non-preferred direction caused a 1.4±0.8% shift (both in the direction of adaptation). The observation that the shift is larger in the preferred direction (although not statistically significant, $p = 0.056$, *t*-test) is consistent with the prediction shown in **Fig. S1c**.

Response latency. The above model assumes that the target neuron and the presynaptic cells have the same response latency, which is important for the development of the asymmetric connections (**Fig. 6**). If the target cell responds with a longer latency than the presynaptic cells, the opposite asymmetry may develop (i.e., some of the "→" cells on the right side of the target neuron may spike before the target neuron, so their connections will be strengthened rather than weakened). However, this is unlikely to be the case. Since the experiments were performed in V1, the target neuron in the model must represent a V1 neuron. As discussed in the main text, the presynaptic neurons are also likely to be in V1. If the presynaptic and the target neurons are indeed from the same

pool, then there should be no systematic difference in their intrinsic response latency (because any presynaptic cell could be the target neuron of another circuit, and vice versa). Alternatively, if the presynaptic cells are not in V1, they must reside in higher cortical areas, because in the thalamocortical pathway direction selectivity first arises in V1. In this case, the presynaptic neurons are likely to exhibit longer latencies than the target neuron in V1, which makes it even less likely for the opposite asymmetry to develop.

References for Supplementary Information:

1. Froemke, R.C. and Dan, Y. Spike-timing-dependent synaptic modification induced by natural spike trains. *Nature* **416**, 433-438 (2002).
2. Felsen, G., Shen, Y.-s., Yao, H., Spor, G., Li, C., and Dan, Y. Dynamic modification of cortical orientation tuning mediated by recurrent connections. *Neuron* **36**, 945-954 (2002).